This is a repository copy of *A finite element assessment of the workpiece plastic deformation in machining of Ti-6Al-4V*.

White Rose Research Online URL for this paper:
https://eprints.whiterose.ac.uk/200319/

Version: Published Version

Proceedings Paper:
Jamshidi, H., Mejías, F.C. and Ghadbeigi, H. orcid.org/0000-0001-6048-9408 (2023) A finite element assessment of the workpiece plastic deformation in machining of Ti-6Al-4V. In: Schulze, V. and Biermann, D., (eds.) Procedia CIRP. 19th CIRP Conference on Modeling of Machining Operations, 31 May - 02 Jun 2023, Karlsruhe, Germany. Elsevier BV , pp. 62-67.

https://doi.org/10.1016/j.procir.2023.03.012

Reuse
This article is distributed under the terms of the Creative Commons Attribution-NonCommercial-NoDerivs (CC BY-NC-ND) licence. This licence only allows you to download this work and share it with others as long as you credit the authors, but you can't change the article in any way or use it commercially. More information and the full terms of the licence here: https://creativecommons.org/licenses/

Takedown
If you consider content in White Rose Research Online to be in breach of UK law, please notify us by emailing eprints@whiterose.ac.uk including the URL of the record and the reason for the withdrawal request.

eprints@whiterose.ac.uk
https://eprints.whiterose.ac.uk/

Available online at www.sciencedirect.com

ScienceDirect

Procedia CIRP 117 (2023) 62–67

www.elsevier.com/locate/procedia

19th CIRP Conference on Modeling of Machining Operations

A Finite Element Assessment of The Workpiece Plastic Deformation in Machining of Ti-6Al-4V

Hamid Jamshidi[a,*], Fernando Cepero Mejías[a], Hassan Ghadbeigi[a]

[a]*The University of Sheffield, Department of Mechanical Engineering, Sir Frederick Mappin Building, Mappin Street, S1 3JD, Sheffield, UK*

* Corresponding author. Tel.: +44 79 60 60 60 18; *E-mail address: h.jamshidi@sheffield.ac.uk*

Abstract

Severe plastic deformation is not desired in machining as it adversely affects surface integrity. In this study, the performance of finite element formulations on subsurface plastic deformation is studied. Finite element models of orthogonal milling of Ti6Al4V have been developed using Update Lagrangian with element deletion as well as continuous remeshing algorithms. The models are validated not only by the measured cutting forces, but quantitative measurements of the subsurface plastic deformation. The results showed that continuous remeshing strategy generate smooth milling forces and predicted the plastic deformation of the machined subsurface with higher accuracy compared to the element deletion method.

© 2023 The Authors. Published by Elsevier B.V.
This is an open access article under the CC BY-NC-ND license (https://creativecommons.org/licenses/by-nc-nd/4.0)
Peer review under the responsibility of the scientific committee of the 19th CIRP Conference on Modeling of Machining Operations

Keywords: machining, milling force, FEM, plastic deformation;

1. Introduction

Severe plastic deformation (SPD) at the machined surface and subsurface has a great influence on the service life of components. Many researchers tried to understand the behavior of the material deformation under high strain, strain rate and high temperature which are inherent characteristics of various machining operations. Early attempts focus on experimental observation [1]. Jeelani and Ramakrishnan [2] used the grid technique to evaluate the strain distribution of the machined surface in an orthogonal test setup. Based on the grid node displacement, they obtained the strain field in the subsurface of a titanium alloy workpiece and concluded that the cutting speed, tool geometry and lubrication are influential parameters [3]. Later more advanced experimental methods were developed to study SPD in high localized plastic deformation zone. For example, Ghadbeigi et al. [4] used electron beam lithography technique to emboss microgrids with a 10 µm pitch and width of 1 µm and successfully measured the strain field very close to the machined surface. Authors in [5] quantified the plastic deformation using the grid technique and linked it with the formation of the white layer in milling of a titanium alloy. Zhang et al. [6] used the digital image correlation (DIC) technique coupled with a thermal infrared imaging to obtain stress and strain fields using a constitutive model in the orthogonal cutting. A pendulum-based cutting test setup was developed by Xu et al. [7] to monitor the chip formation mechanism under varying cutting speed condition. Using this approach, the authors measured the strain contour map of the machined surface of Inconel 718 at various cutting speeds with a single test [7].

Finite Element Modelling (FEM) simulation of the cutting process has also been employed by many researchers to study the machining process. Mir et al. [8] reviewed the simulation approaches and discussed the challenges exist in modelling of plastic deformation at high-strain rate. Li et al. [9] simulated orthogonal cutting of Ti-6Al-4V and validated the simulation results by comparing the chip morphology and cutting force

2212-8271 © 2023 The Authors. Published by Elsevier B.V.
This is an open access article under the CC BY-NC-ND license (https://creativecommons.org/licenses/by-nc-nd/4.0)
Peer review under the responsibility of the scientific committee of the 19th CIRP Conference on Modeling of Machining Operations
10.1016/j.procir.2023.03.012

with the experimental data and then reported the variation of plastic shear strain and the maximum strain rate with the cutting speed. Deng et al. [10] simulated 2D orthogonal cutting test and experimentally studied the chip formation of different metals and showed that how typical shear strain of 2-10 at the shear plain resulted in ultra-fine grain structure of the produced chip. Zhang et al. [11] simulated subsurface deformation of machining of AISI 1045 at various rake angles and reported reasonable results close to the experimental data obtained using the DIC technique.

Based on what has been reviewed, it can be inferred that most experimental and FEM analysis have been conducted based on 2D orthogonal tests where the depth of cut is constant. However, the onset of chip formation and subsequent severe plastic deformation in varying chip load can only be observed under orthogonal milling condition while a reduced process complexity is achieved. Furthermore, a systematic approach is missing from literature to examine different FEM methods and related parameters on SPD in analysis. This study aims to provide more in-depth knowledge on sever plastic deformation of the machined surface and subsurface by simulation of orthogonal milling operation in which the depth of cut varies from zero to the maximum value. The effect of two main formulations i.e. Lagrangian method with element deletion and continuous remeshing algorithm are compared. The effect of FEM parameters especially remeshing parameters are discussed. The FEM results is compared with the experimental data published in [5].

2. Finite Element simulation settings

2D orthogonal milling model was established to resemble the experimental study conducted in [5]. Updated Lagrangian method was used to simulate the process where node coordinates are attached to the material and hence move with the material during deformation. In order to cope with sever mesh distortion and convergence error imposed in this method, adaptive continuous remeshing and element deletion strategies are applied using MSC Marc (Model 1) and Abaqus/Explicit (Model 2) software, respectively.

The powerful remeshing algorithm together with the implicit formulation available in MSC Marc helps to achieve high accuracy predictions at lower computational costs for this type of models. In this context a large increment step time of 10^{-6}s was used in this simulation.

The explicit solver in Abaqus/Explicit, on the other hand, resolves the convergence problems due to the highly nonlinear nature of the model from both materials and boundary conditions perspective. Therefore, it was used to develop and solve the model with element deletion method given the increased computational costs due to the imposed material nonlinearities introduced by damage and failure models. This formulation notably reduces the computational cost allowing the parallel processing and mitigates the convergence problems of the model. The increment time step in this case was reduced to a range between 10^{-8}s and 10^{-9}s to guarantee a high accuracy in the numerical predictions.

Fig. 1(a) shows the model constructed with the continuous remeshing algorithm where three geometrical zones shown as A, B and C were used to control the adaptive remeshing strategy. These follow the tool path with a predetermined threshold for the remeshing process and the element sizes. This strategy allows using finer mesh in high deformation zones while the mesh density can be reduced in other regions. Different mesh sizes were used for zones A and B to investigate the convergence error and accuracy of simulation while the mesh size remain constant (20 μm) in C controlling the mesh density of the tool. 6-node triangular plain strain element type was selected to discretize both bodies. Triangular elements were selected due to their high versatility and consistency of elements aspect ratio in the remeshing zones throughout the simulation. This characteristic is vital to guarantee a high accuracy of the predicted results.

The ''Model 2'' was build using square linear elements with reduced integration CPE4R of $5\,\mu$m in an area 100 microns below the machined surface, as visualized in Fig 1(b). The selected elements accurately predict the local stresses as well as the instant of the element deletion with high precision.

The Johnson-Cook constitutive (Equation 1) was used to represent the material behaviour:

$$\bar{\sigma} = (A + B\varepsilon^{n})\left(1 + C\ln\frac{\dot{\varepsilon}}{\dot{\varepsilon_0}}\right)\left[1 - \left(\frac{T-T_m}{T_r-T_m}\right)^{m}\right] \quad (1)$$

Where $\bar{\sigma}$ is equivalent stress, ε and $\dot{\varepsilon}$ are strain and strain rate respectively and $\dot{\varepsilon_0}$ is the reference strain rate. Element temperature is noted with the variable T. Thermal variables T_m and T_r refer to the melting temperature and reference temperature in the model, respectively. A, B, C, m and n are the empirical constants. All the above variable values are listed in Table 1[12].

Table 1. JC constitutive model constants.

A(MPa)	B(MPa)	C	m	n	T_m(K)	T_r(K)	$\dot{\varepsilon_0}$(1/s)
782.7	498.4	0.028	1.0	0.28	1873	298	0.1

A thermal-structural analysis was used in both software and Table 2 reports the thermal and physical properties of the workpiece and tool used in simulation.

Table 2. Thermal and physical properties of the tool and workpiece material.

Property	Heat Conductivity (W/m.k)	Specific Heat Capacity(J/g°C)	Density (g/cc)	Young's Modulus(GPa)
Tool	110	0.28	19.25	550
Workpiece	7.4	0.52	4.43	110

The failure strain was simulated using the Johnson-cook model as:

$$\bar{\varepsilon_f} = \left(D_1 + D_2 e^{D_3\frac{P}{\bar{\sigma}}}\right)\left(1 + D_4\ln\frac{\dot{\varepsilon}}{\dot{\varepsilon_0}}\right)\left[1 + \left(D_5\frac{T-T_m}{T_r-T_m}\right)^{m}\right] \quad (2)$$

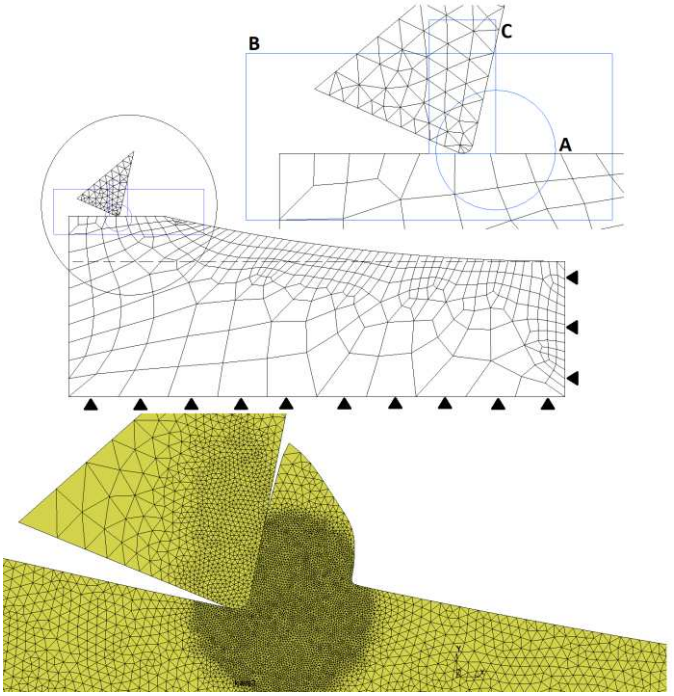

(a)

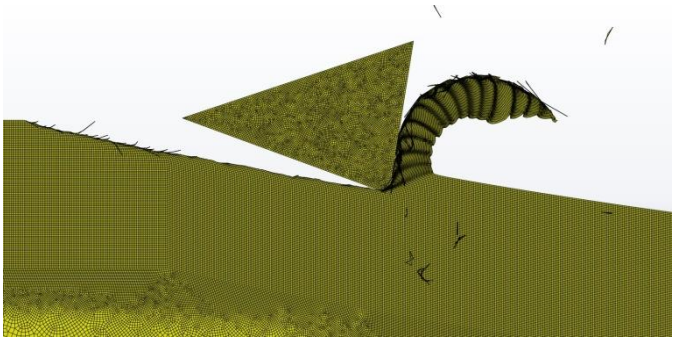

(b)

Fig. 1. Representation of (a) Marc mesh distribution and chip formation and (b) chip formation obtained with element deletion FEM model.

Where $\bar{\varepsilon_f}$ is the fracture strain and P is the hydrostatic pressure, and D_1 to D_5 are constants defined in Table 3 according to [12]. Element damage is predicted by parameter D (equation 3) and the elemental mechanical properties are fully degraded (D=1) when the summation of the incremental equivalent plastic strain ($\Delta\varepsilon_f$) is equal to the fracture strain ($\bar{\varepsilon_f}$), and the element is removed for the model:

$$D = \sum \frac{\Delta\varepsilon_f}{\bar{\varepsilon_f}} \tag{3}$$

Table 3. JC damage model constants.

D_1	D_2	D_3	D_4	D_5
-0.09	0.25	0.5	0.014	3.87

Tool geometry plays a crucial role in chip formation, cutting force and plastic deformation as discussed in [5]. Table 4 shows the tool geometry parameters and cutting conditions used in this study to simulate the experiment conducted in [5].

Table 4. Tool geometry and simulation conditions.

Cutting Speed (m/min).	Radial Depth of cut (mm)	Rake angle	Clearance angle	Edge Radius (μm)	Milling Mode
20	0.5	0	11	30	Down Mill.

Zorev friction model was employed to model the friction behavior in sticking and sliding region in the tool-chip contact length:

$$\begin{cases} \tau(x) = \mu\sigma_n(x) & ,\mu\sigma_n(x) < \tau_{st} \\ \tau(x) = \tau_{st} & ,\mu\sigma_n(x) > \tau_{st} \end{cases} \tag{4}$$

In the above equation, variables $\mu, \boldsymbol{\tau}$ and τ_{st} represent the friction coefficient, shear stress and the ultimate shear stress, respectively. Variable σ_n denotes the normal stress and variable $\boldsymbol{x}$ is the node position along the tool-chip contact interface.

3. Results and Discussion

The formed chip and associated mesh morphology has been shown in Fig. 1. However, the chip forms cannot be validated due to lack of access to the experimentally produced chips. In this section the milling force and machined surface plastic deformation simulation is compared with the experiments.

3.1. Milling force results predictions

A friction coefficient of 0.35 and mesh size of 5 μm and 40 μm was considered in region A and B respectively in continuous remeshing strategy, Figure 1(a). The element size in element deletion approach is 5 μm and the fracture toughness modelled is 12.5 N/mm. The large deformation in the elements within the chip section results a chip with corrugated appearance, as shown in Fig. 1(b). The forces simulated with element deletion show high fluctuations due to the element deletion release abruptly the tool/element contact releasing instantaneously the force exerted by these deleted elements, as shown in Fig. 2. The simulated force however in continuous remeshing strategy show lower fluctuation level due to the remeshing (see Fig. 3).

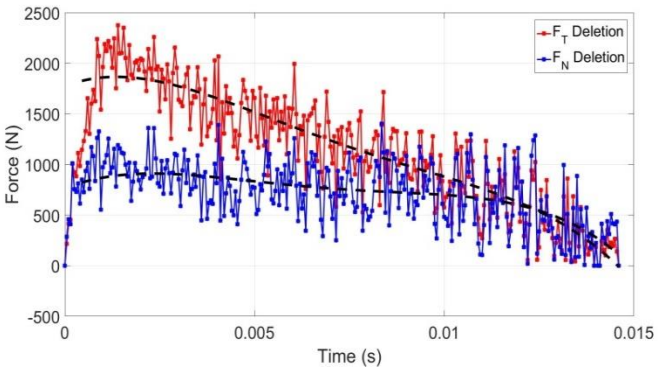

Fig. 2. Machining force predicted using the element deletion approach

Fig. 3 shows tangential (F_T) and normal (F_N) forces obtained from the developed simulations and experiments. Forces predicted by remeshing, and elements deletion techniques show a similar trend. In general, the forces drop faster in FE predictions than in experimental results due to the fact that simulation does not consider a slight tool deflection registered in the trials.

Based on Fig 2 and 3, the FEM with remeshing strategy model can predict the force with a reasonable accuracy compared with element deletion approach.

The peak force values have been used to investigate the effect of adaptive remeshing parameters on the prediction results.

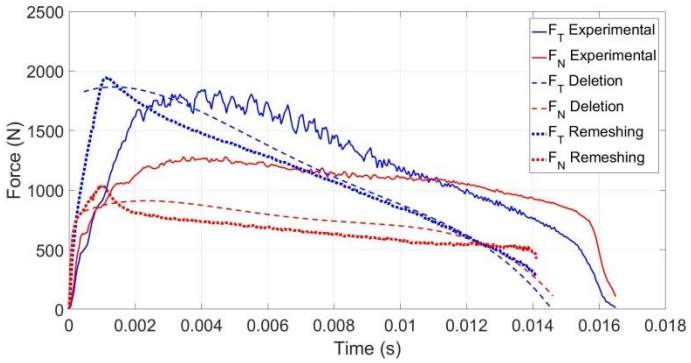

Fig. 3. Simulation and experimental milling force in tangential and normal directions

Fig. 4 shows the effect of element size associated with region A of Figure 1(a) on the maximum tangential and normal force. This region covers the primary, secondary and tertiary shear zones ahead of the tool tip wherein the majority of plastic deformation takes place. The prediction errors increase from 8% to 62%, by increasing the initial element size, 5 µm to 40 µm, applied in the zone.

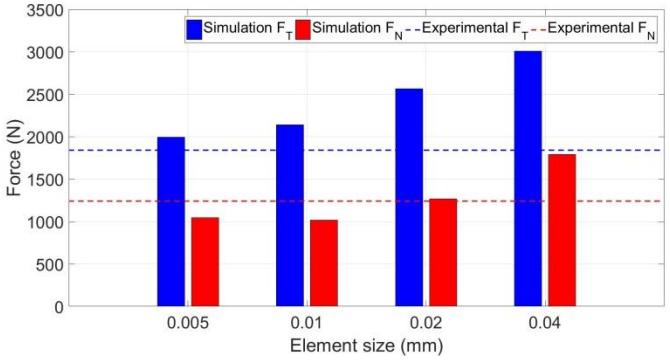

Fig. 4. Effect of element size in continuous adaptive remeshing strategy

However, changing the mesh size in other regions did not change the simulation force. That is because the material is already deformed when it passes through the other regions. therefore, although a single zone may satisfy the prediction accuracy, the transition of a fine to course elements reduces the computation time and virtual gradient of local field parameters. Hence the adaptive remeshing strategy can be applied only on areas of interest to simulate the process without increasing the computational cost. Fig. 4 also demonstrates that the variation of mesh morphology has a more prominent effect on F_T than F_N . Although the initial error in the former was measured to be 8%, this drastically increases to 62% at an initial element size of 40 µm, while the prediction error of F_N varies from 16% to 42 % for the range of applied initial element sizes.

Machining forces predicted from the element deletion model are also very sensitive to the element size. It was found that for element sizes of 5, 10, 20 and 40 microns the forces increase substantially for larger element sizes, as shown in Fig 5. The simulated force using this method is higher than what was measured in the remeshing model when higher element size is used (especially at 20 and 40 micron). Note that the maximum values of the force trend lines are used instead of the force value themselves due to the fact that high force fluctuations create excessive and insignificant force peaks.

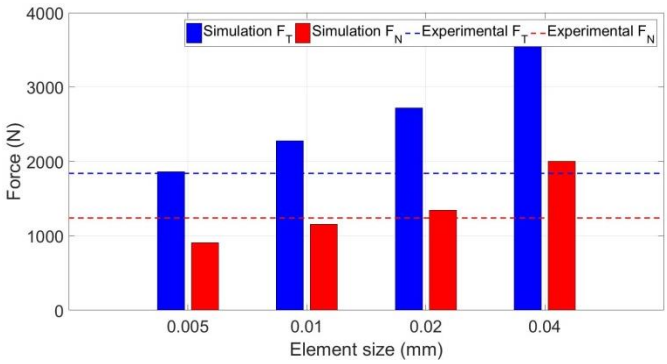

Fig. 5. Effect of element deletion in the element deletion model

Fig. 6 shows the effect of remeshing frequency on the predicted maximum forces where the horizontal axis shows the applied re-meshing increments. Remeshing frequency of 1 indicates that the remeshing strategy is applied after each increment while remeshing frequency of 20 indicates that remeshing strategy is applied every 20 increments.

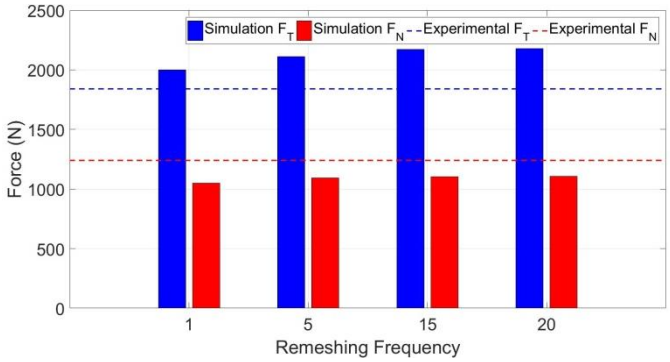

Fig. 6. Effect of remeshing frequency in continuous adaptive remeshing strategy

The predicted forces, both F_T and F_N, are found to be almost insensitive to the remeshing frequency with higher predicted values at longer remeshing intervals with only 7% difference in this case compared with the continuous remeshing. Higher frequencies resulted in convergence error during simulation. Based on these results it can be concluded that the error stays in the same margin of below 10% or reaches the instability due to the severe distortion in case of using heigh remeshing

frequency. This would help to reduce the computation cost while the accuracy is reached. Therefore, less frequent remeshing strategy would be beneficial to reduce the computational cost while the accuracy of the predictions are not significantly affected.

3.2. Machined surface plastic deformation

A 40 µm minimum element size was used in the Model 1 in region B in consistent with the experimental grid size [5]. The true shear strain reached to 80% at the top machined surface while it declined to around 5% at 50 micron below the surface which is the same value reported in the experiments [5]. The plastic deformation on the machined surface and subsurface along the tool path can be observed in Fig. 7.

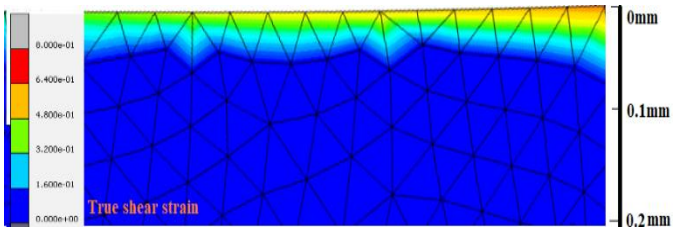

Fig. 7. True shear strain map for the surface machined (minimum element size 0.04mm)

It should be noted that the element size affects the obtained plastic strain. It is observed that the depth with significant plastic strain is substantially reduced for more refined meshes, as shown in Fig. 8. That can be explained by the fact that the smaller elements enhance the prediction's accuracy in local areas.

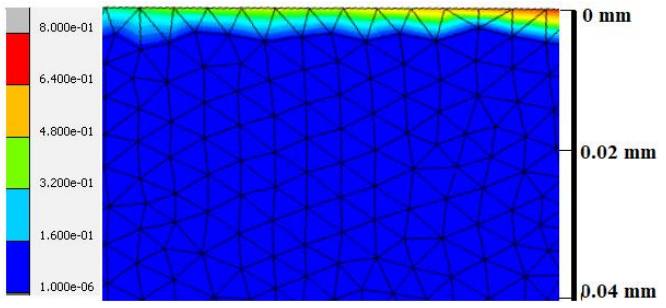

Fig. 8. True shear strain map for the surface machined (element size 0.005mm)

Since elements are removed from the model in Model 2, local force transfer from the removed elements to the subsequent layers is interrupted, preventing the development of large deformations. therefore, the element removal technique becomes inefficient for predicting plastic deformation below the machining surface. Additionally, the cutting tool lose contact with the machined surface when elements are removed, therefore, a large part of the model do not register any deformation (see Fig. 9).

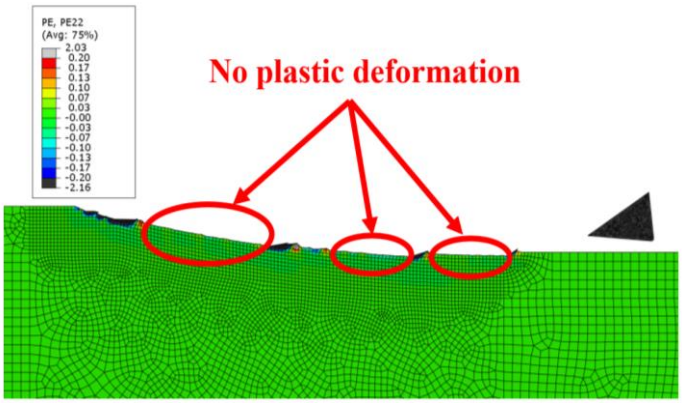

Fig. 9. Plastic deformation in direction y for the deletion element with element size of $40\mu m$

Generally, the predictions obtain with the refined mesh should be used due to their high accuracy. However, in this research a coarse mesh with element size of 40 microns is employed to validate the predicted plastic strains because this is the grid size used in the experiments.

While it was not possible to measure the strain right at the top machined surface in the experiments due to sever grid distortion, the FEM simulation can measure the strain at top surface. Fig. 10 shows the predicted xx, yy and xy components of strain profile from the machined surface until 0.25 mm beneath the surface. The result of simulation shows that the strain in x and y direction at the machined surface can reach to 1.28 and -1.28 which is very high to be captured experimentally. The strain rate profile shows that the depth of plastically deformed layer reaches to around 100 µm versus a thickness of 75 µm observed from the experiments [5]. The strain value in x direction 50 µm beneath the surface is approximately 0.22 and -0.22 in y direction. While the simulation results in y direction is in good agreement with the experimental data reported in [5] (0.20) the value in x and xy directions are smaller in the experiments (around 0.05) which need further investigation on the cause of error in these directions.

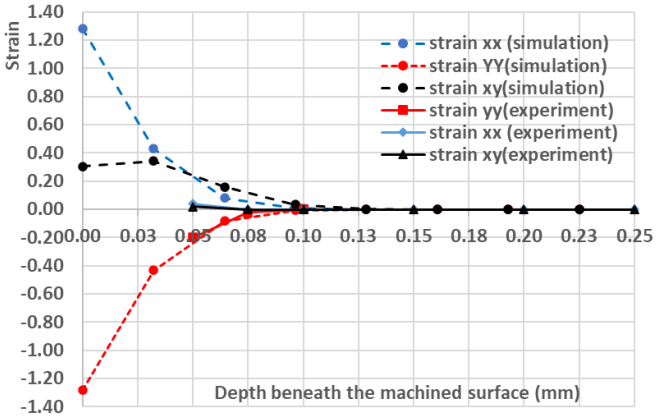

Fig. 10. Simulation strain profile beneath the machined surface

4. Conclusions

This paper aims to simulated 2D orthogonal milling process and investigate the plastic deformation of the

machined surface and subsurface. The performance of two simulation approaches namely element deletion and continuous remeshing methods were studied. The type of formulations showed little effect on the performance of FE model of the chip formation in the studied problem. It is concluded that the continuous remeshing strategy simulated the milling force with less fluctuation compared to the element deletion method and predicted the depth of plastic deformation with a reasonable accuracy. In addition, the remeshing strategy are computationally more efficient (increment step time of 10^{-6}s vs 10^{-8}s to 10^{-9}s used in element deletion method) with less sensitivity to the element size. The remeshing frequency found to have minimal effect within the convergence limit of the model. The element removal technique is inefficient for predicting plastic deformation below the machining surface due to the force interruption transmission caused by deletion of the elements. As a result, the remeshing algorithm is the most effective way to predict the subsurface deformation after machining owing to the continuum nature of the model. The simulated strain values using the remeshing strategy shows that the depth of plastically deformed layer reaches to around 100 μm which is 25% higher the experimentally measured layer. Furthermore, the strain value in x direction was simulated with 10% discrepancy with the experiment while higher error obtained in other directions which needs further investigations.

Acknowledgements

This research was funded as part of the SENSYCUT project by EPSCR (EP/v055011/1)

References

[1] T.H.C. Childs, A new visio-plasticity technique and a study of curly chip formation, Int. J. Mech. Sci. 13 (1971) 373–387. https://doi.org/10.1016/0020-7403(71)90061-0.

[2] S. Jeelani, K. Ramakrishnan, Subsurface plastic deformation in machining annealed 18% ni maraging steel, Wear. 81 (1982) 263–273. https://doi.org/10.1016/0043-1648(82)90275-7.

[3] S. Jeelani, K. Ramakrishnan, Subsurface plastic deformation in machining 6Al-2Sn-4Zr-2Mo titanium alloy, Wear. 85 (1983) 121–130. https://doi.org/10.1016/0043-1648(83)90340-X.

[4] H. Ghadbeigi, S.R. Bradbury, C. Pinna, J.R. Yates, Determination of micro-scale plastic strain caused by orthogonal cutting, Int. J. Mach. Tools Manuf. 48 (2008) 228–235. https://doi.org/10.1016/j.ijmachtools.2007.08.017.

[5] M. Brown, R. M'Saoubi, P. Crawforth, A. Mantle, J. McGourlay, H. Ghadbeigi, On deformation characterisation of machined surfaces and machining-induced white layers in a milled titanium alloy, J. Mater. Process. Technol. 299 (2022) 117378. https://doi.org/10.1016/j.jmatprotec.2021.117378.

[6] D. Zhang, X.M. Zhang, H. Ding, A Study on the Orthogonal Cutting Mechanism Based on Experimental Determined Displacement and Temperature Fields, Procedia CIRP. 46 (2016) 35–38. https://doi.org/10.1016/j.procir.2016.03.176.

[7] D. Xu, Z. Liao, D. Axinte, M. Hardy, A novel method to continuously map the surface integrity and cutting mechanism transition in various cutting conditions, Int. J. Mach. Tools Manuf. 151 (2020) 103529. https://doi.org/10.1016/j.ijmachtools.2020.103529.

[8] A. Mir, X. Luo, I. Llavori, A. Roy, D.L. Zlatanovic, S.N. Joshi, S. Goel, Challenges and issues in continuum modelling of tribology, wear, cutting and other processes involving high-strain rate plastic deformation of metals, J. Mech. Behav. Biomed. Mater. 130 (2022). https://doi.org/10.1016/j.jmbbm.2022.105185.

[9] A. Li, J. Pang, J. Zhao, J. Zang, F. Wang, FEM-simulation of machining induced surface plastic deformation and microstructural texture evolution of Ti-6Al-4V alloy, Int. J. Mech. Sci. 123 (2017) 214–223. https://doi.org/10.1016/j.ijmecsci.2017.02.014.

[10] W.J. Deng, W. Xia, C. Li, Y. Tang, Formation of ultra-fine grained materials by machining and the characteristics of the deformation fields, J. Mater. Process. Technol. 209 (2009) 4521–4526. https://doi.org/10.1016/j.jmatprotec.2008.10.043.

[11] D. Zhang, S. Zhao, X.-M. Zhang, H. Ding, Machining subsurface deformation under various rake angles, Procedia CIRP. 108 (2022) 863–867. https://doi.org/10.1016/j.procir.2022.05.200.

[12] S. Zhu, J. Liu, X. Deng, Modification of strain rate strengthening coefficient for Johnson-Cook constitutive model of Ti6Al4V alloy, Mater. Today Commun. 26 (2021) 102016. https://doi.org/10.1016/j.mtcomm.2021.102016.